

# Effect of Helium on Mechanical Properties of High Chromium ODS Ferritic/Martensitic Steels for Fusion Applications

著者	Hasegawa A, Kakinuma N, Nogami S, Satou M, Abe K, Kasada R, Kimura A, Jitsukawa S
journal or publication title	CYRIC annual report
volume	2007
page range	21-24
year	2007
URL	<a href="http://hdl.handle.net/10097/44380">http://hdl.handle.net/10097/44380</a>

### III. 1. Effect of Helium on Mechanical Properties of High Chromium ODS Ferritic/Martensitic Steels for Fusion Applications

*Hasegawa A.<sup>1</sup>, Kakinuma N.<sup>1</sup>, Nogami S.<sup>1</sup>, Satou M.<sup>1</sup>, Abe K.<sup>1</sup>,  
Kasada R.<sup>2</sup>, Kimura A.<sup>2</sup>, and Jitsukawa S.<sup>3</sup>*

<sup>1</sup>*Department of Quantum Science and Energy Engineering, Tohoku University*

<sup>2</sup>*Institute of Advanced Energy, Kyoto University*

<sup>3</sup>*Japan Atomic Energy Agency*

#### Introduction

The reduced activation ferritic/martensitic (RAFM) steels are one of the candidate structural materials for fusion reactor<sup>1)</sup>. In the fusion reactor environment, 14 MeV neutron irradiation might produce displacement damage and transmutant helium (He) atoms in structural materials. For instance, the displacement damage will be 100 dpa and He concentration will be 1000 appm in RAFM steel after 10 MW/m<sup>2</sup> neutron wall loading. The displacement damage might cause an irradiation hardening at temperature below 400°C and the irradiation hardening might reduce fracture toughness, which includes a ductile brittle transient temperature (DBTT) shift to higher temperatures<sup>1)</sup>. It is well known that He might stabilize a point defect cluster and cause the additional hardening at lower temperature region and the increase of swelling at higher temperature region. He atoms in material might diffuse to form He bubbles at the preexisting grain boundary during higher temperature irradiation and tend to change the fracture mode from the transgranular fracture to the intergranular fracture. The previous study<sup>2)</sup> in our group showed the excellent resistance of the ODS (oxide dispersion strengthened) RAFM steel against He accumulation at higher temperature. Almost no change of the DBTT and non-intergranular fracture of the 9Cr (9% Chromium)-ODS steel were observed after He implantation up to 1000 appm at 550°C using the Cyclotron accelerator of CYRIC.

Higher Cr content in the ODS steel than 9% is considered to be effective to suppress corrosion in fusion reactor coolant<sup>3)</sup>. The objective of this study is to investigate the effect of He at high temperature on mechanical properties of the high-Cr ODS steel using high energy  $\alpha$ -particle irradiation by the Cyclotron accelerator.

## Experimental

The material used in this study was the 14Cr-ODS ferritic/martensitic steel, which was fabricated by a mechanical alloying (MA) process. The chemical composition of this material is shown in Table 1. This material includes high density ultra fine oxides, which were produced from original  $Y_2O_3$  powders during the MA process and the following heat treatment ( $1050^\circ\text{C} \times 1 \text{ h}$  for tempering). Miniaturized Charpy V notch (CVN) specimen for the Charpy impact test was machined with the dimension of  $1.5 \text{ mm} \times 1.5 \text{ mm} \times 20 \text{ mm}$  and the notch geometry of 0.3 mm in notch depth, 0.08 mm in notch root radius and  $30^\circ$  in notch angle. Figure 1 shows the CVN specimen shape and geometry.

He-ion implantation was performed using 50 MeV  $\alpha$ -particles from the AVF cyclotron of CYRIC of Tohoku University. The projected range of 50 MeV He-ions in a Fe-9Cr steel was calculated to be about 400  $\mu\text{m}$  by TRIM code<sup>4)</sup>. The tandem type energy degrader system consisting of 2 rotating wheels was used to obtain the uniform depth distribution of He atoms in specimens<sup>5)</sup>. The calculated depth distribution of He concentration and displacement damage is shown in Fig. 2. The nominal He concentration was about 1000 appm. The displacement damage was about 0.37 dpa at the specimen surface and 0.28 dpa in average. The implantation temperature was  $550^\circ\text{C} \pm 10^\circ\text{C}$ , which was measured using thermocouples during the implantation test.

The Charpy impact property evaluation and the fracture surface analysis after the impact test were carried out after He implantation. The Charpy impact test was carried out using an instrumented Charpy impact testing equipment at the Hot Laboratory of International Research Center for Nuclear Materials Science of Tohoku University. The test temperature ranged from  $-146^\circ\text{C}$  to room temperature. The fracture surface of the CVN specimens after the impact test was observed using a scanning electron microscope (SEM) at the same laboratory.

## Results and discussion

The Charpy impact data of the 14Cr-ODS steel is shown in Fig. 3. Almost no increment of the DBTT after He implantation at  $550^\circ\text{C}$  was observed. The DBTT of the 14Cr-ODS steel before/after He implantation was about  $-110^\circ\text{C}$ , which was about  $60^\circ\text{C}$  lower than that of the 9Cr-ODS steel before/after He implantation. Almost no change of the upper shelf of the absorbed energy after He implantation was also observed. The upper shelf of the absorbed energy of the 14Cr-ODS steel was about 0.7 J before/after He

implantation, which was about 0.2 J higher than that of the 9Cr-ODS steel before/after He implantation. The typical fracture surfaces for the He-implanted Charpy impact specimen of the 14Cr-ODS steel tested at  $-146^{\circ}\text{C}$  is shown in Fig. 4. Fracture mode for the He-implanted region was the same as the He-unimplanted region, which was cleavage fracture.

The Charpy impact properties (DBTT, upper shelf of the absorbed energy) of the 14Cr-ODS steel were relatively good in comparison with that of the 9Cr-ODS steel. Since the 14Cr-ODS steel also showed higher resistance against the corrosion than the 9Cr-ODS steel as mentioned above, the 14Cr-ODS steel might be more adequate as the structural material for fusion reactor based on these experimental results.

### Acknowledgement

The authors are grateful to the staffs of CYRIC of Tohoku University relating to the accelerator operation and the irradiation experiments. This work was partly supported by the JUPITER-II (Japan-USA Program of Irradiation Testing for Fusion Research II) program.

### References

- 1) Baluc N., Gelles D.S., Jitsukawa S., Kimura A., Klueh R.L., Odette G.R., van der Schaaf B., Yu Jinnan., *J. Nucl. Mater.* **367-370** (2007) 33.
- 2) Hasegawa A., Ejiri M., Nogami S., Satou M., Abe K., Kimura A., Jitsukawa S., *CYRIC Annual Report* (2006) 19.
- 3) Cho H.S., Kimura A., *J. Nucl. Mater.* **367-370** (2007) 1180.
- 4) Biersack J.P., Ziegler J.F., *TRIM85 Program*, IBM Corp., Yorktown, NY, 1985.
- 5) Hasegawa A., Wakabayashi E., Tanaka K., Abe K., Jitsukawa S., *CYRIC Annual Report* (2002) 34.

Table 1. The chemical composition of the 14Cr-ODS ferritic steel (unit: wt.%).

C	Si	Mn	Cr	W	N	Ti	Al	Y <sub>2</sub> O <sub>3</sub>	Fe
0.04	0.033	0.06	13.64	1.95	0.009	0.28	4.12	0.381	Bal.

1.5mm Center V Notched Specimen (1.5CVN)

Figure 1. The shape and geometry of the miniaturized Charpy V notch (CVN) specimen.

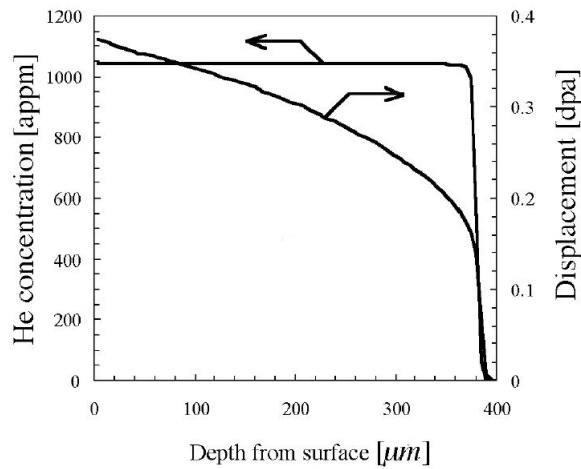


Figure 2. The calculated depth distribution of He concentration and displacement damage in the 14Cr-ODS steel..

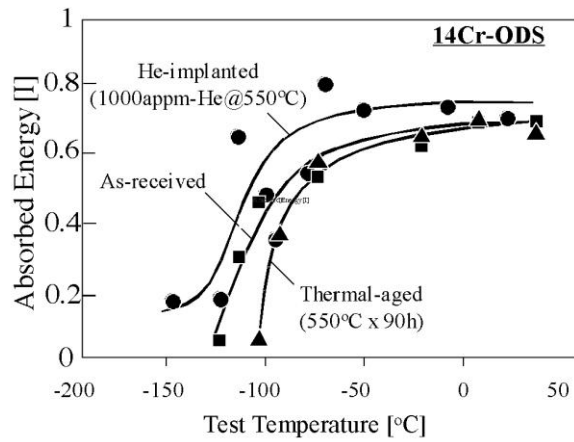


Figure 3. The Charpy impact data for the 14Cr-ODS steel..

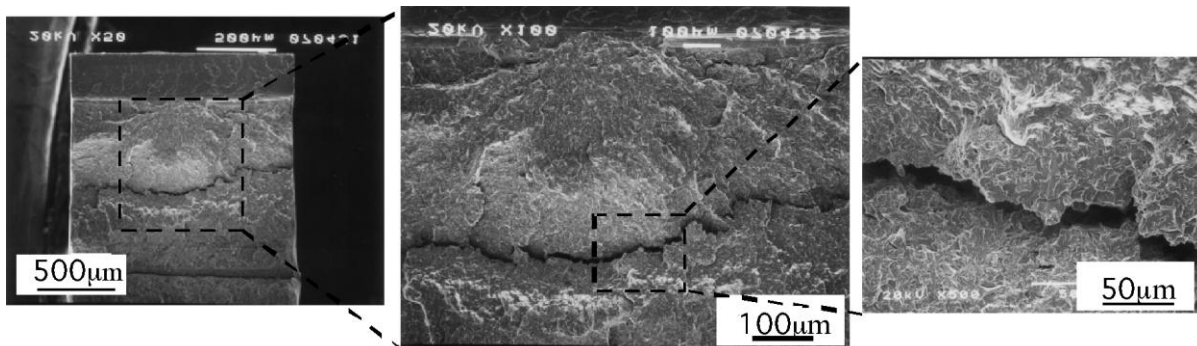


Figure 4. The typical fracture surfaces for the He-implanted Charpy impact specimen of the 14Cr-ODS steel tested at  $-146^{\circ}\text{C}$ .